International Journal of Information, Control and Computer Sciences
ISSN: 2517-9942
Vol:2, No:9, 2008

Systholic Boolean Orthonormalizer Network in Wavelet Domain for Microarray Denoising

Mario Mastriani

***Abstract*—**We describe a novel method for removing noise (in wavelet domain) of unknown variance from microarrays. The method is based on the following procedure: We apply 1) Bidimentional Discrete Wavelet Transform (DWT-2D) to the Noisy Microarray, 2) scaling and rounding to the coefficients of the highest subbands (to obtain integer and positive coefficients), 3) bit-slicing to the new highest subbands (to obtain bit-planes), 4) then we apply the Systholic Boolean Orthonormalizer Network (SBON) to the input bit-plane set and we obtain two orthonormal otput bit-plane sets (in a Boolean sense), we project a set on the other one, by means of an AND operation, and then, 5) we apply re-assembling, and, 6) re-scaling. Finally, 7) we apply Inverse DWT-2D and reconstruct a microarray from the modified wavelet coefficients. Denoising results compare favorably to the most of methods in use at the moment.

***Keywords*—**Bit-Plane, Boolean Orthonormalization Process, Denoising, Microarrays, Wavelets

I. Introduction

A microarray is affected by noise in its acquisition and processing. Microarray denoising is used to remove the additive noise while retaining as much as possible the important image features. In the recent years there has been an important amount of research on wavelet thresholding and threshold selection for bioimages denoising, e.g., microarray images [1], [2], because wavelet provides an appropriate basis for separating noisy signal from the image signal. The motivation is that as the wavelet transform is good at energy compaction, the small coefficients are more likely due to noise and large coefficient due to important signal features [3]-[5]. These small coefficients can be thresholded without affecting the significant features of the image.

In general, the results of the microarray processing combine two sample images that after further image processing, gene expression data can be produced for further analysis, such as gene clustering or identification [1], [2]. These three crucial steps, experiment, image processing and data analysis, determine the success or not of the microarray analysis. Image processing plays a potentially large impact on the subsequent analysis. In recent years, a large number of commercial tools have been developed in microarray image processing [1], [2]. The tasks of all these tools mainly focus on two major targets, namely: spot segmentation and spot intensity extraction. However, the quality of the images from the experiments is not always perfect. The gene array experiments involve a large number of error-prone steps which lead to a high level of noise in the resulting images [1], [2]. Hence, the accuracy of the gene expressions derived from these images will largely be affected in the process.

In order to assure the accuracy of the gene expression, normally the replicated experiments and incorporated statistical methods are needed to estimate the errors [1], [2]. These methods deal mainly with measurement error, such as preparation of the sample, cross hybridization, and fluctuation of fluorescence value from gene to gene. But none deals particularly with the effect of the noise [1], [2].

In fact, the thresholding technique is the last approach based on wavelet theory to provide an enhanced approach for eliminating such noise source and ensure better gene expression. Thresholding is a simple non-linear technique, which operates on one wavelet coefficient at a time. In its basic form, each coefficient is thresholded by comparing against threshold, if the coefficient is smaller than threshold, set to zero; otherwise it is kept or modified. Replacing the small noisy coefficients by zero and inverse wavelet transform on the result may lead to reconstruction with the essential signal characteristics and with less noise. Since the work of Donoho & Johnstone [5], there has been much research on finding thresholds, however few are specifically designed for images [3], [4], [6].

Unfortunately, this technique has the following disadvantages:

1) it depends on the correct election of the type of thre-sholding, e.g., OracleShrink, VisuShrink (soft-thresholding, hard-thresholding, and semi-soft-thresholding), Sure-Shrink, Bayesian soft thresholding, Bayesian MMSE estimation, Thresholding Neural Network (TNN), due to Zhang, NormalShrink, , etc. [3]-[7],
2) it depends on the correct estimation of the threshold which is arguably the most important design parameter,
3) it doesn't have a fine adjustment of the threshold after their calculation,
4) it should be applied at each level of decomposition, needing several levels, and
5) the specific distributions of the signal and noise may not be well matched at different scales.

Therefore, a new method without these constraints will represent an upgrade.

Manuscript received December 28, 2005.

The author is with the SAOCOM Mission, National Commission of Space Activities (CONAE), 751 P. Colon Ave., 5th Floor, C1063ACH Buenos Aires, Argentina (e-mail: mmastri@conae.gov.ar). Tel: (54-11) 4331 0074 Ext. 221.

The Bidimensional Discrete Wavelet Transform and the method to reduce noise by wavelet thresholding is outlined in Section II. The SBON as an Boolean orthonormalizer and as a denoiser tool in wavelet domain is outlined in Section III. In Section IV, we discuss briefly the noise sources and its statistical measurement in microarray imaging. In Section V, the experimental results using the proposed algorithm are presented. Finally, Section VI provides a conclusion of the paper.

II. Bidimensional Discrete Wavelet Transform

The Bidimensional Discrete Wavelet Transform (DWT-2D) [8]-[17] corresponds to multiresolution approximation expressions. In practice, mutiresolution analysis is carried out using 4 channel filter banks composed of a low-pass and a high-pass filter and each filter bank is then sampled at a half rate (1/2 down sampling) of the previous frequency. By repeating this procedure, it is possible to obtain wavelet transform of any order. The down sampling procedure keeps the scaling parameter constant (equal to ½) throughout successive wavelet transforms so that is benefits for simple computer implementation. In the case of an image, the filtering is implemented in a separable way be filtering the lines and columns.

Note that [8] the DWT of an image consists of four frequency channels for each level of decomposition. For example, for *i*-level of decomposition we have:
$LL_{n,i}$: Noisy Coefficients of Approximation.
$LH_{n,i}$: Noisy Coefficients of Vertical Detail,
$HL_{n,i}$: Noisy Coefficients of Horizontal Detail, and
$HH_{n,i}$: Noisy Coefficients of Diagonal Detail.

The LL part at each scale is decomposed recursively, as illustrated in Fig. 1.

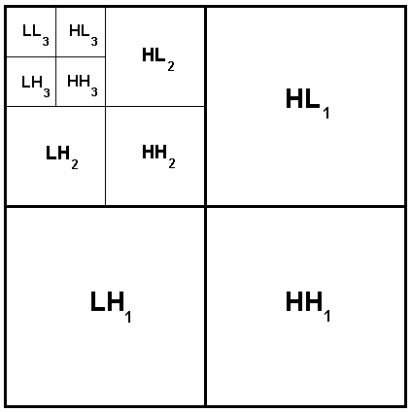

Fig. 1 Data preparation of the image. Recursive decomposition of LL parts

To achieve space-scale adaptive noise reduction, we need to prepare the 1-D coefficient data stream which contains the space-scale information of 2-D images. This is somewhat similar to the "zigzag" arrangement of the DCT (Discrete Cosine Transform) coefficients in image coding applications [18]. In this data preparation step, the DWT-2D coefficients are rearranged as a 1-D coefficient series in spatial order so that the adjacent samples represent the same local areas in the original image. An example of the rearrangement of an 8-by-8 transformed image is shown in Fig. 2, which will be referred to as a 1D space-scale data stream.

Each number in Fig. 2 represents the spatial order of the 2D coefficient at that position corresponding to Fig. 1.

64	63	15	45	3	9	33	39
62	61	30	60	6	12	36	42
14	44	13	43	18	24	48	54
29	59	28	58	21	27	51	57
2	8	32	38	1	7	31	37
5	11	35	41	4	10	34	40
17	23	47	53	16	22	46	52
20	26	50	56	19	25	49	55

Fig. 2 Data preparation of the image. Spatial order of 2-D coefficients

A. Wavelet Noise Thresholding

The wavelet coefficients calculated by a wavelet transform represent change in the image at a particular resolution. By looking at the image in various resolutions it should be possible to filter out noise. At least in theory. However, the definition of noise is a difficult one. In fact, "one person's noise is another's signal". In part this depends on the resolution one is looking at. One algorithm to remove Gaussian white noise is summarized by D.L. Donoho and I.M. Johnstone [5], and synthesized in Fig. 3.

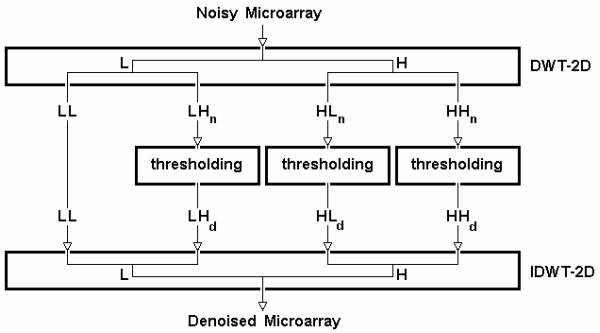

Fig. 3 Thresholding Techniques

The algorithm is:

1) Calculate a wavelet transform and order the coefficients by increasing frequency. This will result in an array containing the image average plus a set of coefficients of length 1, 2, 4, 8, etc. The noise threshold will be calculated on the highest frequency coefficient spectrum (this is the largest spectrum).

2) Calculate the *median absolute deviation* on the largest coefficient spectrum. The median is calculated from the absolute value of the coefficients. The equation for the median absolute deviation is shown below:

$$\delta_{mad} = \frac{median(|\ C_{n,i}\ |)}{0.6745} \quad (1)$$

where $C_{n,i}$ may be $LH_{n,i}$, $HL_{n,i}$, or $HH_{n,i}$ for *i*-level of decomposition. The factor 0.6745 in the denominator rescales the numerator so that δ_{mad} is also a suitable estimator for the standard deviation for Gaussian white noise [5].

3) For calculating the noise threshold λ we have used a modified version of the equation that has been discussed in papers by D.L. Donoho and I.M. Johnstone. The equation is:

$$\lambda = \delta_{mad}\sqrt{2log[N]} \quad (2)$$

where N is the number of pixels in the subimage, i.e., HL, LH or HH.

4) Apply a thresholding algorithm to the coefficients. There are two popular versions:
4.1. Hard thresholding. Hard thresholding sets any coefficient less than or equal to the threshold to zero, see Fig. 4 (a).

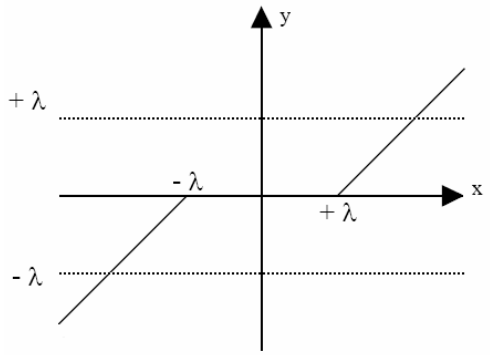

Fig. 4 (a) Soft-Thresholfing

where ***x*** may be $LH_{n,i}$, $HL_{n,i}$, or $HH_{n,i}$, ***y*** may be $HH_{d,i}$:
Denoised Coefficients of Diagonal Detail,
$HL_{d,i}$: Denoised Coefficients of Horizontal Detail,
$LH_{d,i}$: Denoised Coefficients of Vertical Detail,
for *i*-level of decomposition.

The respective code is:

```
for row = 1:N^1/2
  for column = 1:N^1/2
    if |Cn,i[row][column]| <= λ,
      Cn,i[row][column] = 0.0;
    end
  end
end
```

4.2. Soft thresholding. Soft thresholding sets any coefficient less than or equal to the threshold to zero, see Fig. 4(b). The threshold is subtracted from any coefficient that is greater than the threshold. This moves the image coefficients toward zero.

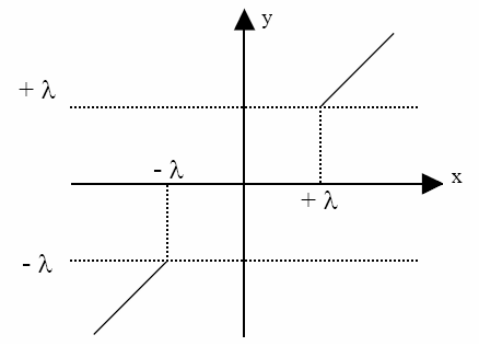

Fig. 4 (b) Hard-Thresholfing

The respective code is:

```
for row = 1:N^1/2
  for column = 1:N^1/2
    if |Cn,i[row][column]| <= λ,
      Cn,i[row][column] = 0.0;
    else
      Cn,i[row][column] = Cn,i[row][column] - λ;
    end
  end
end
```

III. Synthetic Boolean Orthonormalizer Network

The SBON was introduced by Mastriani [19] as a Boolean Orthonormalization Process (*BOP*) to convert a non-orthonormal Boolean basis, i.e., a set of non-orthonormal binary vectors (in a Boolean sense) to an orthonormal Boolean basis, i.e., a set of orthonormal binary vectors (in a Boolean sense). The BOP algorithm has a lot of fields of applications, e.g.: Steganography, Hopfield Networks, Boolean Correlation Matrix Memories, Bi-level image processing, lossy compression, iris, fingerprint and face recognition, improving edge detection and image segmentation, among others. That is to say, all those applications that need orthonormality in a Boolean sense. It is important to mention that the BOP is an extremely stable and fast algorithm.

A. Orthonormality in a Boolean Sense

Given a set of binary vectors $\mathbf{u}_k$ = [$\mathbf{u}_{k1}$, $\mathbf{u}_{k2}$, … , $\mathbf{u}_{kp}$]^T (where k = 1, 2, … , q, and [.]^T means transpose of [.]), *they are orthonormals in a Boolean sense*, if they satisfy the following pair of conditions:

$$u_k \wedge u_j = u_k = u_j \text{ if } k = j \quad (3.1)$$

and

$$u_k \wedge u_j = 0 \text{ if } k \neq j \quad (3.2)$$

where $0 = [\,0\,,\,0\,,\,\ldots\,,\,0\,]^T$, and the term $u_k \wedge u_j$ represents the *AND operation between each element of the binary vectors* u_k and u_j , i.e.,

$$u_k \wedge u_j = [u_{k1} \wedge u_{j1}\,,\, u_{k2} \wedge u_{j2}\,,\, \bullet\bullet\bullet\,,\, u_{kp} \wedge u_{jp}\,]^T \qquad (4)$$

B. Boolean Orthonormalization Process (BOP)

Given a set of key binary vectors that are nonorthonormal (in a Boolean sense), we may use a *preprocessor* to transform them into an orthonormal set (in a Boolean sense); the preprocessor is designed to perform a *Boolean orthonormalization* on the key binary vectors prior to association. This form of transformation is described below, maintaining a one-to-one correspondence between the input (key) binary vectors v_1 , v_2 , $\ldots$, v_N , the resulting orthonormal binary vectors u_1 , u_2 , $\ldots$, u_N , and the residual binary vectors s_1 , s_2 , $\ldots$, s_N .

1) Version 1: As it is shown in the Fig. 5

$$s_i = v_i \veebar u_i \quad \forall\ i\,,\ \text{with } s_1 = 0 \qquad (5)$$

$$u_i \wedge s_i = 0 \quad \forall\ i \qquad (6)$$

where $\veebar$ represents the XOR operation. Eq.(6) represents the orthogonality principle in a Boolean sense [19].

$$u_i \wedge u_k = 0 \quad \forall\ i \neq k \qquad (7)$$

$$s_{i,j} \leq v_{i,j} \quad \forall\ i\,,j \qquad (8)$$

Algorithm:

$u_j = v_j \quad \forall\ j$

$u_j = u_j \veebar (v_j \wedge u_i),\ \ i \in [1, j\text{-}1],\ j \in [1, N]$

2) Version 2: As it is shown in the Fig. 6

$$u_i = v_i \veebar s_i \quad \forall\ i\,,\ \text{with } u_1 = v_1\,,\ \text{because } s_1 = 0 \qquad (9)$$

Algorithm:

$s_j = 0 \quad \forall\ j$

$s_j = s_j \vee (v_j \wedge (v_i \veebar s_i)\,),\ \ i \in [1, j\text{-}1],\ j \in [1, N]$

C. SBON in wavelet domain for microarray denoising

The new method of microarray denoising can be represented by the Fig. 7, according to the following algorithm:

We apply
1) DWT-2D to the Noisy Microarray,

2) scaling and rounding to the coefficients of the highest subbands (for to obtain integer and positive coefficients),

3) bit-slicing to the new highest subbands (for to obtain bit-planes), see Fig. 8
4) SBON to the input bit-plane set and we obtain two orthonormal otput bit-plane sets (in a Boolean sense), we project a set on the other one, by means of an AND operation, and then, see Fig. 9

5) re-assembling, and, see Fig. 8

6) re-scaling, and

7) Inverse DWT-2D and reconstruct a microarray from the modified wavelet coefficients.

IV. Noise Sources and its Statistical Measurement in Microarray Imaging

It is well known microarray technology can monitor thousand of DNA sequences in a high density array on a glass. The basic procedure for a microarray experiment is simply described as follow. Two mRNA samples are reverse-transcribed into cDNA, labeled using different fluorescent dyes (e.g., the red fluorescent dye Cy5 and the green fluorescent dye Cy3), then mixed and hybridized with the arrayed *DNA* sequences. After this competitive hybridization, the slides are imaged using a scanner which makes fluorescence measurement for each dye. From the differential hybridization of the two samples, the relative abundance of the spotted *DNA* sequences can be assessed. A schematic diagram for this process created is shown in [2].

The results of the microarray experiment are two 16-bit tagged mage files, one for each fluorescent dye. The Fig. 10(a) show an example of the mentioned microarray image. As shown in Fig. 10(b), the image is not perfect and it includes noisy sources that blur such image for further gene expression experimentation. The noise source originates from different sources during the course of experiment, such as photon noise, electronic noise, laser light reflection, dust on the slide, and so on. Hence, it is crucial to denoise the resultant image within this process.

Exciting methods to reduce the noise source include using clean glass slide and using a higher laser power rather than higher PMT voltages. However, there are not adequate for the required image qualities and an enhanced software procedure embedded within the process in a much better alter-native. In this paper, we focus on the implementation of the *SBON* method (in wavelet domain) to the denoising on microarray images [2]. Yet there are some fundamental obstacles that need clarification before the full potential of microarrays can be explored. One of the major problems in interpre-tation of microarray data is that different clustering techniques produce different results.

On the other hand, the assessment parameters that are used to evaluate the performance of noise reduction [20], [21] are the following ones:

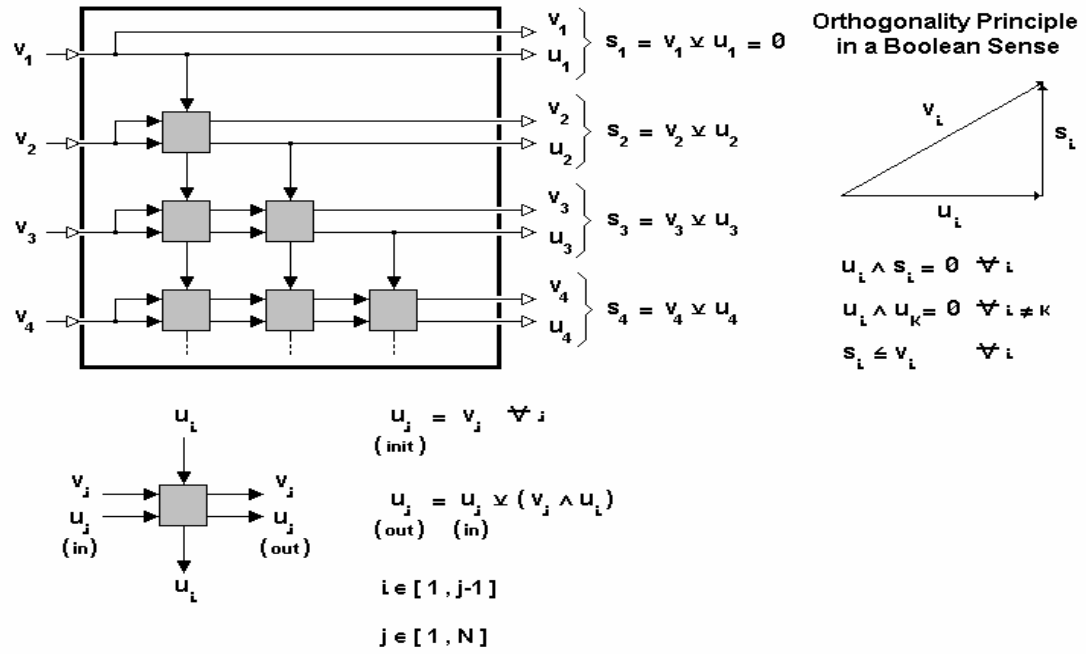

Fig. 5 SBON, version 1

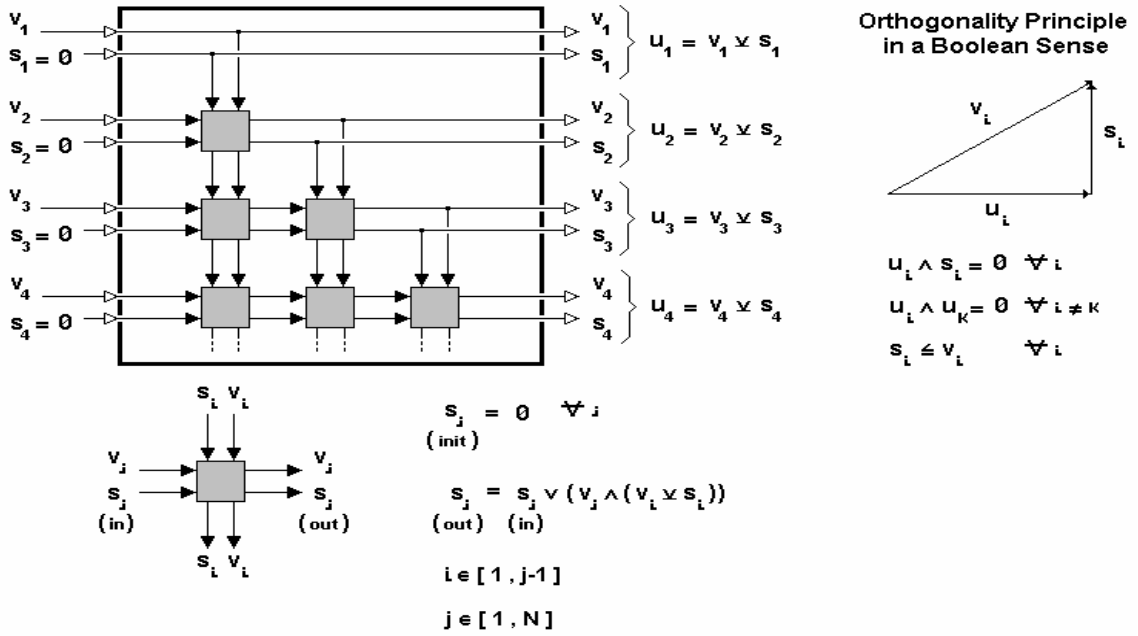

Fig. 6 SBON, version 2

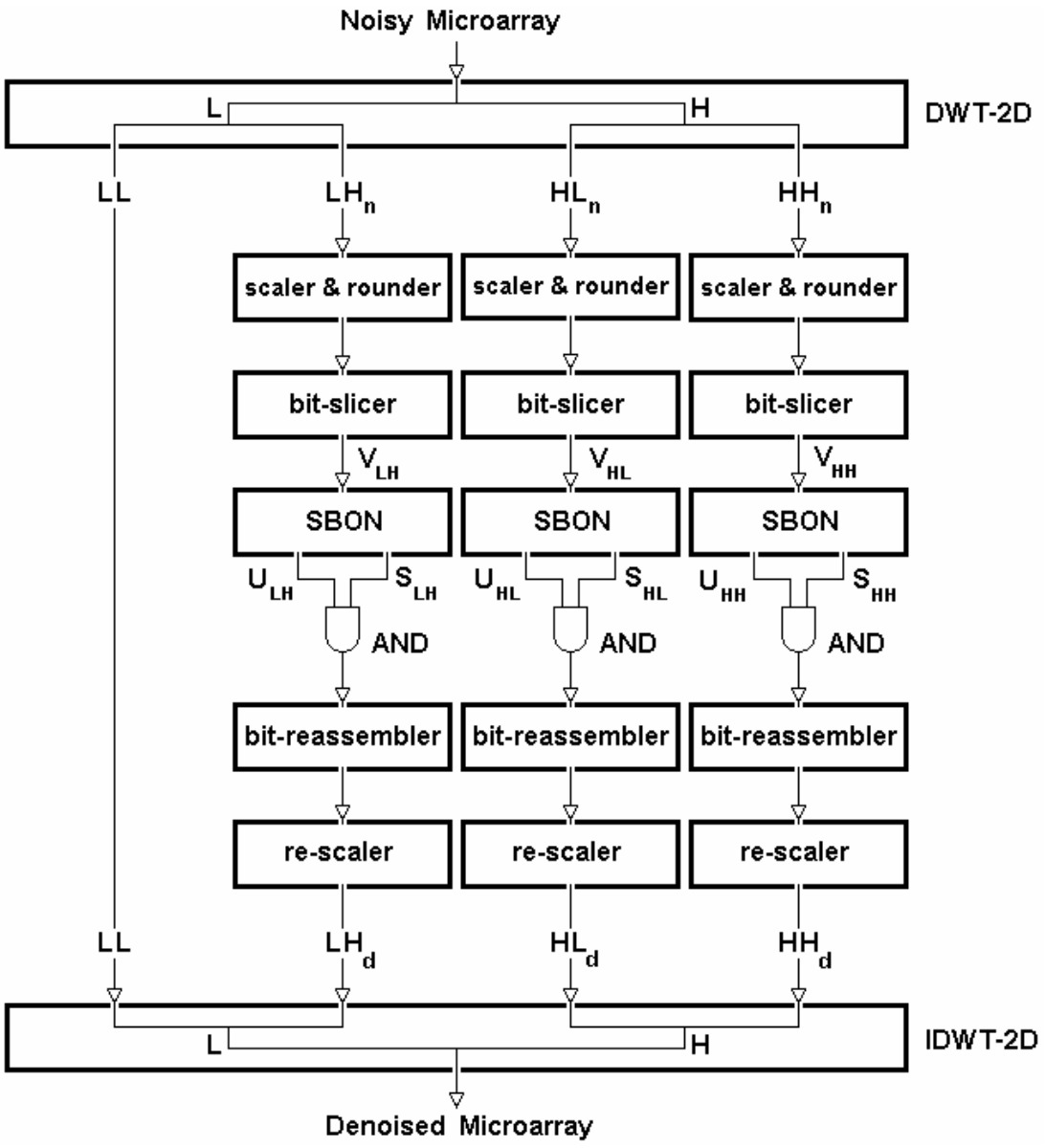

Fig. 7 Microarray denoising

Average Absolute Difference (AAD):

$$AAD = \frac{\sum_{r,c} \left| I(r,c) - I_d(r,c) \right|}{R*C} \quad (10)$$

Signal to Noise Ratio (SNR):

$$SNR = \frac{\sum_{r,c} I(r,c)^2}{\sum_{r,c} (I(r,c) - I_d(r,c))^2} \quad (11)$$

Peak Signal to Noise Ratio (PSNR):

$$PSNR = \frac{R * C * \max_{r,c}(I(r,c)^2)}{\sum_{r,c} (I(r,c) - I_d(r,c))^2} \quad (12)$$

Image Fidelity (IFy):

$$IFy = 1 - \frac{1}{SNR} \quad (13)$$

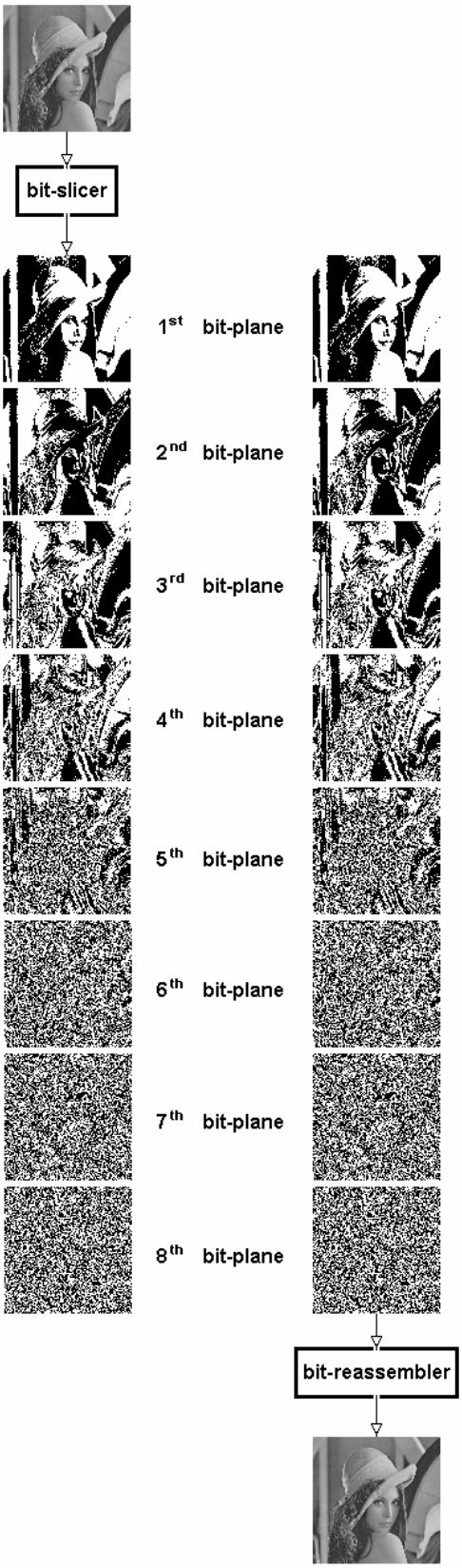

Fig. 8 Lena's bit-slicing and re-assembling.

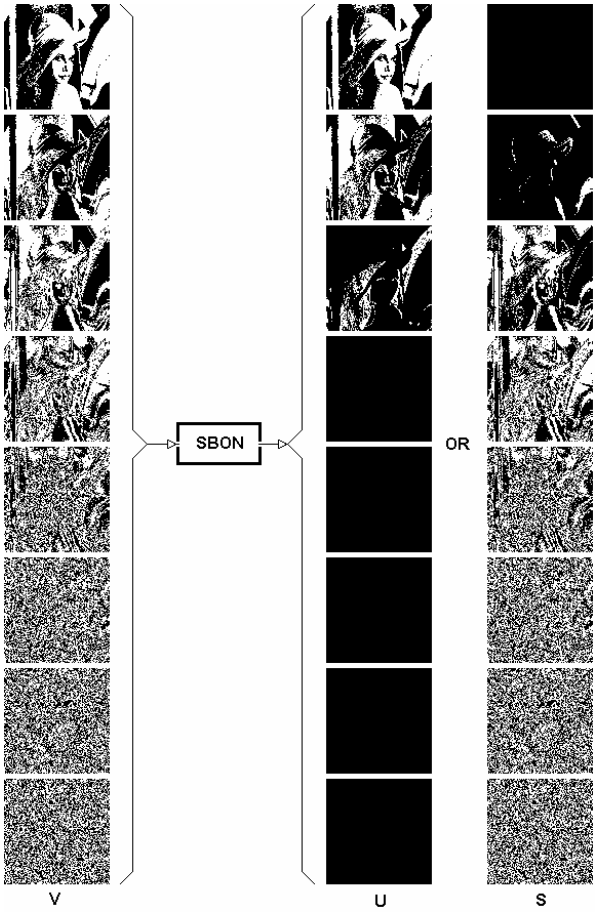

Fig. 9 SBON application on Lena's bit-plane set

Correlation Quality (CQy):

$$CQy = \frac{\sum_{r,c} I(r,c) * I_d(r,c)}{\sum_{r,c} I(r,c)} \tag{14}$$

Structural Content (SCt):

$$SCt = \frac{\sum_{r,c} I(r,c)^2}{\sum_{r,c} I_d(r,c)^2} \tag{15}$$

Where for an image of *R*C* (rows-by-columns) pixels, *r* means row, *c* means column, *I* means original image (without noise), and I_d means denoised image. Such as, a lower *AAD* gives a "cleaner" image as more noise is reduced; larger *SNR* and *PSNR* indicates a smaller difference between the original (without noise) and denoised image; if *IFy* and *SCt* spread at 1, we will obtain an image I_d of better quality; and a larger

value of *CQy* usually corresponds to a better quantitative performance [20], [21].

On the other hand, to compare edge preservation performances of different noise reduction schemes, we adopt the Pratt's figure of merit (*FOM*) [21] defined by

$$FOM = \frac{1}{max\{\hat{N}, N_{ideal}\}} \sum_{i=1}^{\hat{N}} \frac{1}{1 + d_i^2 \alpha} \tag{16}$$

where $\hat{N}$ and N_{ideal} are the number of detected and ideal edge pixels, respectively, d_i is the Euclidean distance between the *i*th detected edge pixel and the nearest ideal edge pixel, and α is a constant typically set to 1/9. *FOM* ranges between 0 and 1, with unity for ideal edge detection.

V. Results

The simulations demonstrate that the SBON technique improves the noise reduction performance to the maximum, for bioimages. Here, we present a set of experimental results using two bioimages. Such images were converted to bitmap file format for their treatment [22].

For statistical filters employed, i.e., Median, Lee, Kuan, Gamma-Map, Enhanced Lee, Frost, Enhanced Frost, Wiener, DS, and EDS, we use a reduction scheme [22]. Figure 10 shows the noisy (30 %) and filtered microarray images used in the first experiment of [1], with a 274-by-274 (pixels) by 65536 (gray levels) bitmap matrix. Table 1 summarizes the assessment parameters vs. 19 filters for Fig. 10, where En-Lee means Enhanced Lee Filter, En-Frost means Enhanced Frost Filter, ST means Soft-Thresholding, HT means Hard-Thresholding and SST means Semi-Soft-Thresholding.

The assessment parameters were applied to the whole image.

Figure 11 shows the noisy (10 %) and filtered microarray images used in the second experiment of [1], with a 256-by-256 (pixels) by 65536 (gray levels) bitmap matrix. Table 2 summa-rizes the assessment parameters vs. 19 filters for Figure 11. In both cases, the bioimages were processed by using 10 statistical filters, VisuShrink with Daubechies 4 wavelet basis and 1 level of decomposition (improvements were not noticed with other basis of wavelets) [2], [3], [5], [6], [22], SureShrink, Oracle-Shrink, BayesShrink, NormalShrink, TNN [5]-[7], [22], and SBON respectively. Figures 10 and 11 summarize the edge preservation performance of the SBON technique vs. the rest of the filters with a considerably acceptable computational complexity. A 3-by-3 kernel was employed for all statistic noise filters. For *TNN* [7] the empirical function parameter value $\lambda = 0.01$.

For Lee, Enhanced Lee, Kuan, Gamma, Frost and Enhanced Frost filters the damping factor is set to 1, see [3], [22]. The quantitative results of Table 1 and 2 shows that the *SBON* technique can eliminate noise without distorting useful image information and without destroying the important image edges.

Also, in the experiment, the *SBON* outperformed the conventional and no conventional noise reducing filters in terms of edge preservation measured by Pratt figure of merit [21]. In nearly every case in every homogeneous region, the *SBON* produced the lowest standard deviation and was able to preserve the mean value of the region.

The numerical results are further supported by qualita-tive examination, as shown in Fig. 10 and 11.

On the other hand, all filters was applied to complete image, for Figure 10 (274-by-274) pixels and Figure 11 (256-by-256) pixels, and all the filters were implemented in MATLAB® (Mathworks, Natick, MA) on a PC with an Athlon (2.4 GHz) processor.

VI. Conclusions

In this paper we have developed a *SBON* technique based tools for removing additive noise in microarrays. The simulations show that the *SBON* have better performance than the most commonly used filters for microarrays (for the studied benchmark parameters) which include statistical filters, wavelets, and a version of *TNN*. The *SBON* exploits the local coefficient of variations in reducing noise. The performance figures obtained by means of computer simulations reveal that the *SBON* technique provides superior performance in comparison to the above mentioned filters in terms of smoothing uniform regions and preserving edges and features. The effectiveness of the technique encourages the possibility of using the approach in a number of ultrasound and radar applications. Besides, the method is computationally efficient and can significantly reduce the noise while preserving the resolution of the original microarray image. Considerably increased Pratt's figure of merit strongly indicates improvement in detection performance. Also, cleaner images suggest potential improvements for classification and recognition. On the other hand, the drawback of applying the developed SBON technique for removing additive noise in microarrays is the increase in the computational complexity, for blame of the slicing process.

Finally, the natural extension of this work is in Synthetic Aperture Radar (SAR) images, as well as in multimedial applications.

Acknowledgment

The author thanks Prof. Silvano Zanutto, Director of the Biomedical Engineering Institute, at University of Buenos Aires for his help and support.

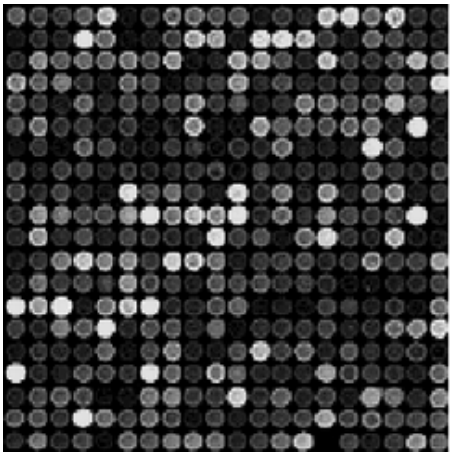

original

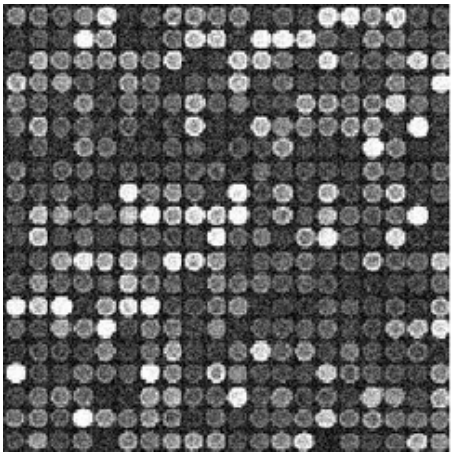

noisy

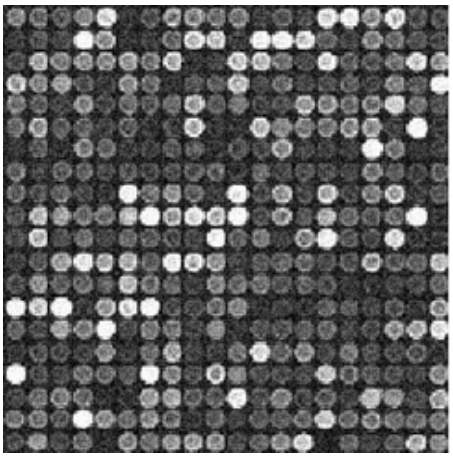

SBON

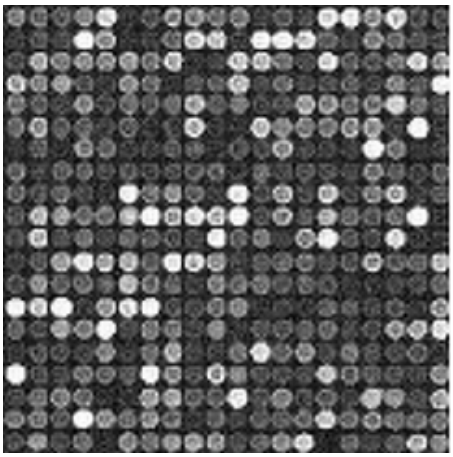

SUREShrink

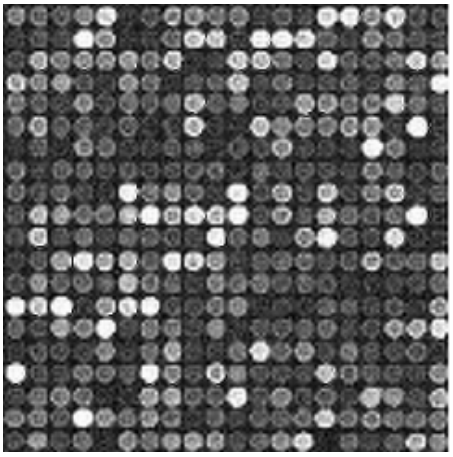

BayesShrink

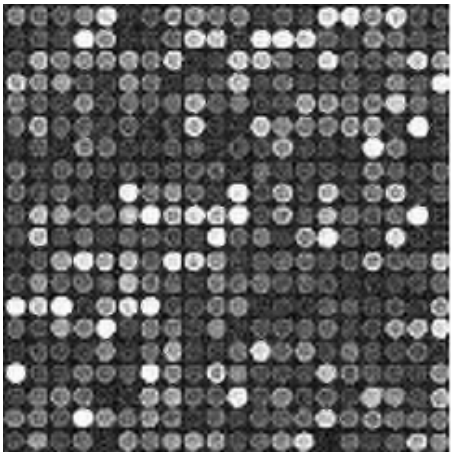

NormalShrink

Fig. 10 Original, noisy and filtered images

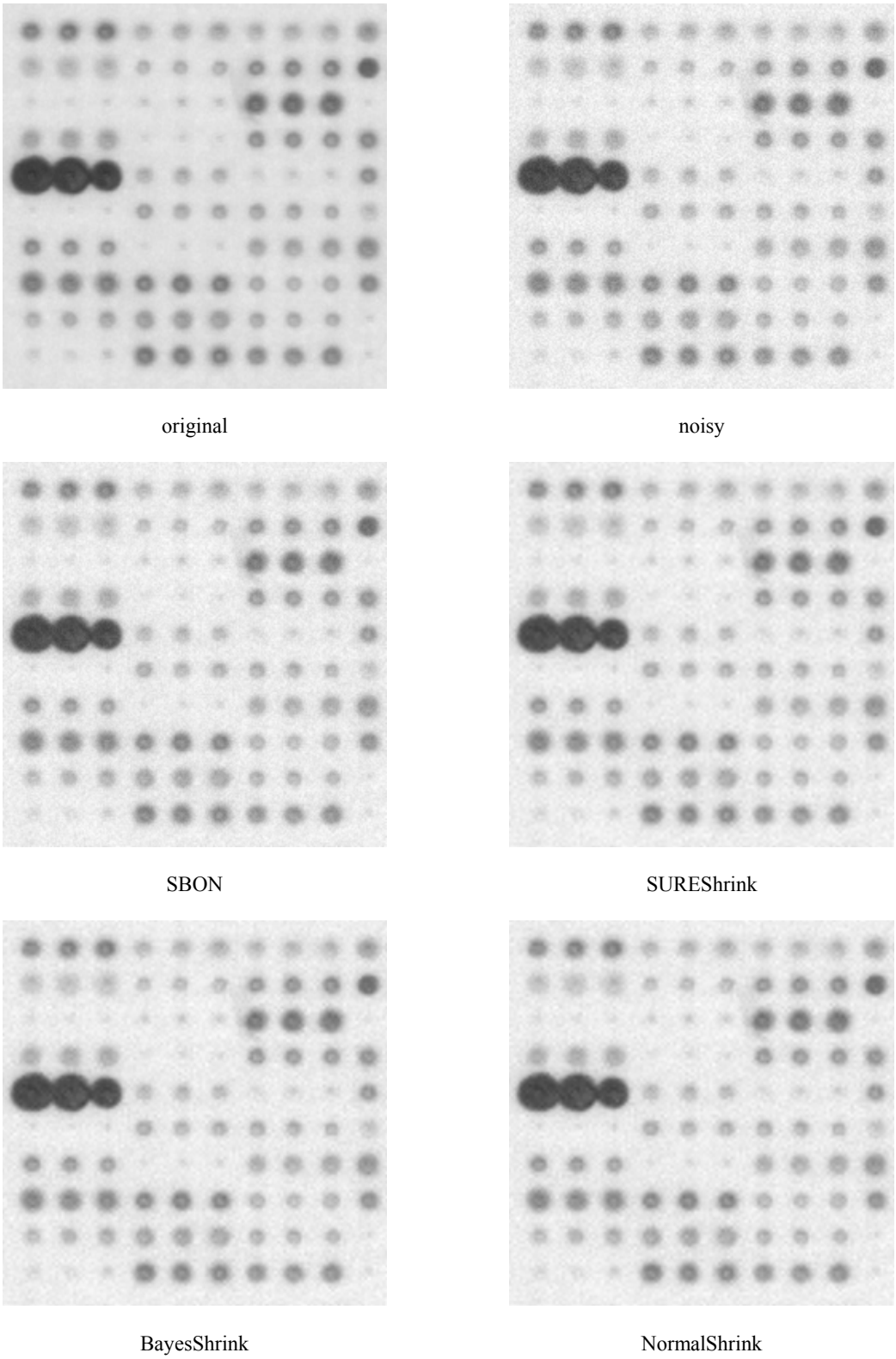

Fig. 11 Original, noisy and filtered images

TABLE I
ASSESSMENT PARAMETERS VS. FILTERS FOR FIGURE 10

Filter	Assessment Parameter						
	AAD	SNR	PSNR	IF	CQ	SC	FOM
En-Frost	38.2653	3.4464	33.7364	0.7109	150.7467	0.5663	0.39857
En-Lee	39.7437	3.3363	33.8373	0.7112	150.7472	0.5632	0.49876
Frost	38.4374	3.2423	33.7033	0.7106	150.5244	0.5689	0.48756
Lee	39.2427	3.4242	32.6363	0.7015	150.4141	0.5924	0.43447
Gamma	39.6252	3.1112	33.2703	0.7063	150.1918	0.5751	0.44235
Kuan	39.8224	3.1243	31.8272	0.7041	149.3121	0.5715	0.45342
Median	39.5252	3.1131	32.7916	0.6852	148.9172	0.5896	0.40704
Wiener	39.1829	3.4557	33.7033	0.7106	150.5244	0.5689	0.44236
DS	38.7332	3.4657	33.9997	0.7169	150.9898	0.5599	0.64111
EDS	38.1484	3.6969	34.1315	0.7182	151.5252	0.5612	0.64324
VisuShrink (ST)	39.1450	3.4596	33.7412	0.7109	151.1527	0.5657	0.44382
VisuShrink (HT)	38.8612	3.5283	34.4115	0.7166	151.3316	0.5666	0.44324
VisuShrink (SST)	38.1829	3.5557	34.7033	0.7196	151.9202	0.5612	0.46432
SureShrink	38.1612	3.5751	34.7193	0.7198	151.9244	0.5611	0.43322
OracleShrink	38.1189	3.6957	34.7233	0.7198	151.9844	0.5619	0.45534
BayesShrink	38.1145	3.6968	34.7237	0.7199	151.9953	0.5612	0.46329
NormalShrink	38.1098	3.6998	34.8734	0.7199	151.9983	0.5609	0.59333
TNN	38.1008	3.7157	34.8833	0.7199	151.9992	0.5600	0.65432
SBON	37.7155	3.7772	36.8388	0.7353	155.4613	0.5513	0.69123

TABLE II
ASSESSMENT PARAMETERS VS. FILTERS FOR FIGURE 11

Filter	Assessment Parameter						
	AAD	SNR	PSNR	IF	CQ	SC	FOM
En-Frost	12.4747	290.1324	363.6712	0.9830	226.4744	0.8972	0.41265
En-Lee	12.8474	290.2522	363.9321	0.9883	226.8373	0.8932	0.51986
Frost	12.1847	290.2772	363.0233	0.9828	226.3272	0.8923	0.55312
Lee	12.3733	290.2333	363.0238	0.9838	226.2822	0.8943	0.44421
Gamma	12.3830	290.8331	363.3433	0.9882	226.8383	0.8934	0.51235
Kuan	12.3833	290.8272	363.4923	0.9887	226.8381	0.8934	0.54129
Median	12.9973	289.1212	361.8374	0.9673	225.9287	0.8734	0.51286
Wiener	11.9042	290.8635	363.5568	0.9866	226.8901	0.8954	0.56413
DS	11.4572	290.9950	363.9393	0.9898	226.9723	0.8993	0.64213
EDS	11.5792	290.9998	363.9865	0.9899	226.9975	0.8993	0.64449
VisuShrink (ST)	11.9055	289.2367	361.5523	0.9761	222.7564	0.8872	0.51228
VisuShrink (HT)	11.9042	290.8673	363.5615	0.9966	226.8909	0.8976	0.56424
VisuShrink (SST)	11.7864	290.9546	363.9822	0.9975	226.8937	0.8984	0.56389
SureShrink	11.7074	291.0753	363.8343	0.9991	226.8942	0.8991	0.57432
OracleShrink	11.8436	290.9332	363.7363	0.9968	226.8963	0.8983	0.55234
BayesShrink	11.9353	290.9363	363.7361	0.9923	226.8942	0.8962	0.56328
NormalShrink	11.6875	290.9992	363.9353	0.9992	226.9021	0.8999	0.59611
TNN	11.4447	291.7243	363.9991	0.9994	226.9732	0.9002	0.62900
SBON	10.9071	294.9237	383.1090	0.9992	229.8972	0.9173	0.69322

REFERENCES

[1] E.C. Rouchka. (2004, April). Lecture 12: Microarray Image Analysis. [Online]. Available: http://kbrin.a-bldg.louisville.edu/CECS694/Lecture12.ppt

[2] X.H. Wang, S.H. Istepanian, and Y.H. Song, "Microarray Image Enhancement by Denoi-sing Using Stationary Wavelet Transform," *IEEE Transactions on Nanobioscience*, vol.2, no. 4, pp.184-189, December 2003. [Online]. Available: http://technology.kingston.ac.uk/momed/papers/IEEE_TN_Micorarray_Wavelet%20Denoising.pdf

[3] H.S. Tan. (2001, October). Denoising of Noise Speckle in Radar Image. [Online]. Available: http://innovexpo.itee.uq.edu.au/2001/projects/s804294/thesis.pdf

[4] H. Guo, J.E. Odegard, M. Lang, R.A. Gopinath, I. Selesnick, and C.S. Burrus, "Speckle reduction via wavelet shrinkage with application to SAR based ATD/R," Technical Report CML TR94-02, CML, Rice University, Houston, 1994.

[5] D.L. Donoho and I.M. Johnstone, "Adapting to unknown smoothness via wavelet shrinkage," *Journal of the American Statistical Association*, vol. 90, no. 432, pp. 1200-1224, 1995.

[6] S.G. Chang, B. Yu, and M. Vetterli, "Adaptive wavelet thresholding for image denoising and compression," *IEEE Transactions on Image Processing*, vol. 9, no. 9, pp.1532-1546, September 2000.

[7] X.-P. Zhang, "Thresholding Neural Network for Adaptive Noise reduction," *IEEE Trans. on Neural Networks*, vol.12, no. 3, pp.567-584, May 2001.

[8] I. Daubechies, *Ten Lectures on Wavelets*, SIAM, Philadelphia, 1992.

[9] B.B. Hubbard, *The World According to Wavelets: The Story of a Mathematical Technique in the Making*, A. K. Peter Wellesley, Massachusetts, 1996.

[10] S. G. Mallat, "Multiresolution approximations and wavelet orthonormal bases of L2 (R)," *Transactions of the American Mathematical Society*, 315(1), pp.69-87, 1989a.

[11] A. Grossman and J. Morlet, "Decomposition of Hardy Functions into Square Integrable Wavelets of Constant Shape," *SIAM J. App Math*, 15: pp.723-736, 1984.

[12] C. Valens. (2004). A really friendly guide to wavelets. [Online]. Available:http://perso.wanadoo.fr/polyvalens/clemens/wavelets/wavelets.html

[13] G. Kaiser, *A Friendly Guide To Wavelets*, Boston:Birkhauser, 1994.
[14] I. Daubechies, "Different Perspectives on Wavelets," in *Proceedings of Symposia in Applied Mathematics*, vol. 47, American Mathematical Society, USA, 1993.
[15] J. S. Walker, *A Primer on Wavelets and their Scientific Applications*, Chapman & Hall/CRC, New York, 1999.
[16] E. J. Stollnitz, T.D. DeRose, and D.H. Salesin, *Wavelets for Computer Graphics: Theory and Applications*, Morgan Kaufmann Publishers, San Francisco, 1996.
[17] J. Shen and G. Strang, "The zeros of the Daubechies polynomials," in *Proc. American Mathematical Society,* 1996.
[18] A.K. Jain, *Fundamentals of Digital Image Processing,* Englewood Cliffs, New Jersey, 1989.
[19] M. Mastriani, *"Enhanced Boolean Correlation Matriz Memory",* (RNL02), in *Proceedings of* X RPIC Reunión de Trabajo en Procesamiento de la Información y Control, San Nicolás, Buenos Aires, Argentina, October 8-10, 2003.
[20] G. Delfino and F. Martinez. (2000, March). Watermarking insertion in digital images (spanish). [Online]. Available: http://www.internet.com.uy/fabianm/watermarking.pdf
[21] Y. Yu, and S.T. Acton, "Speckle Reducing Anisotropic Diffusion," *IEEE Trans. on Image Processing*, vol. 11, no. 11, pp.1260-1270, 2002.
[22] M. Mastriani and A. Giraldez, "Enhanced Directional Smoothing Algorithm for Edge-Preserving Smoothing of Synthetic-Aperture Radar Images," *Journal of Measurement Science Review*, vol 4, no. 3, pp.1-11, 2004. [Online]. Available: http://wwwmeasurement.sk/2004/S3/Mastriani.pdf

Prof. Mario Mastriani was born in Buenos Aires, Argentina on February 1, 1962. He is Professor of Digital Signal and Image Processing in Biomedicine of Faculty of Engineering, at Buenos Aires University (UBA). He is working in the speckle filter of the first synthetic aperture radar (SAR) satellite of SAOCOM Mission, National Commission of Space Activities (CONAE), Buenos Aires, Argentina. He published 39 papers. He is a currently reviewer of IEEE Transactions on Neural Networks, Signal Processing Letters, Transactions on Image Processing, Transactions on Signal Processing, Communications Letters, Transactions on Geoscience and Remote Sensing, Transactions on Medical Imaging, Transactions on Biomedical Engineering, Transactions on Fuzzy Systems, Transactions on Multimedia; Springer-Verlag Journal of Digital Imaging; and SPIE Optical Engineering Journal.
His areas of interest include Digital Signal Processing, Digital Image Processing, wavelets and Neural Networks.